Article

Not peer-reviewed version

Induction of Embryogenic Callus, Protoplast Isolation, and PEG-Mediated Transformation Protocols in *Eucommia ulmoides*

Hongrun Zhou , Zibo Zhou , Jiangyuan Zhang , Haoran Kan , Menggi Yin , Han Zhang , Luyao Wang , Jie Zhao * , Jing Ye *

Posted Date: 23 December 2025

doi: 10.20944/preprints202512.2044.v1

Keywords: *Eucommia ulmoides*; embryogenic callus; protoplast isolation; transient transformation

 doi:10.20944/preprints202512.2044.v1

Article

Induction of Embryogenic Callus, Protoplast Isolation, and PEG-Mediated Transformation Protocols in *Eucommia ulmoides*

Hongrun Zhou [1], Zibo Zhou [1], Jiangyuan Zhang [2], Haoran Kan [2], Mengqi Yin [1], Han Zhang [1], Luyao Wang [1], Jie Zhao [2,*] and Jing Ye [1,2,*]

[1] Laboratory of Forestry Department, Agricultural College, Shihezi University, Shihezi, China

[2] Key Laboratory of Xinjiang for Oasis Agricultural Pests Management and Plant Protection Resources Utilization, Agriculture College, Shihezi University, Shihezi, China

* Correspondence: zhaojie198967@163.com (J.Z.); yejing_shz@foxmail.com (J.Y.)

Abstract

Eucommia ulmoides, a tree species native to China, holds considerable medicinal, ecological, and industrial importance. However, the absence of an efficient and stable genetic transformation system poses significant challenges to gene function studies and molecular breeding in *E. ulmoides*. Protoplasts, which lack cell walls, serve as effective receptors for transient transformation and are thus ideal for genetic engineering research. In this study, we identified the optimal conditions for callus induction using a full-factorial experimental design and accurately identified embryogenic callus through paraffin sectioning. Furthermore, we developed an efficient protoplast isolation and PEG-mediated transient transformation system using embryogenic callus as the starting material. Our findings revealed that the optimal medium for inducing embryogenic callus was B5, supplemented with 1.5 mg/L 6-BA, 0.5 mg/L NAA, 30 g/L sucrose, and 7 g/L agar. This medium achieved a callus induction rate of 97.50% and an embryogenic callus induction rate of 86.30%. For protoplast isolation, the best conditions involved enzymatic digestion with 1.5% cellulase R-10 and 1.0% macerozyme R-10 at an osmotic pressure of 0.6 M for 4 h, resulting in 1.82×10^6 protoplasts/g FW with 91.13% viability. The highest transfection efficiency (53.23%) was attained when protoplasts were cultured with 10 μg of plasmid and 40% PEG4000 for 20 min. This study successfully established a stable and efficient system for protoplast isolation and transient transformation in *E. ulmoides*, offering technical support for exploring somatic hybridization and transient gene expression in this species.

Keywords: *Eucommia ulmoides*; embryogenic callus; protoplast isolation; transient transformation

1. Introduction

Eucommia ulmoides Oliv., a distinctive economic tree species native to China, holds considerable medicinal, ecological, and industrial significance [1,2]. The bark and leaves of *E. ulmoides* are abundant in bioactive compounds like iridoids, lignans, and flavonoids, which have impressive pharmacological properties, including anti-inflammatory effects, blood pressure regulation, and bone metabolism modulation [3–5]. In the industrial sector,

Eu-rubber stands out as a unique bio-based polymer resource in China, emerging as a natural polymer material. Predominantly found in the bark, stems, leaves, seeds, and other tissues of *E. ulmoides* [6,7], this polymer offers a strategic alternative to natural rubber [3,8]. Furthermore, *E. ulmoides* demonstrates robust tolerance to abiotic stresses such as cold and drought, making it a valuable model for exploring stress resistance mechanisms and secondary metabolism regulation in woody plants [9–11].

 doi:10.20944/preprints202512.2044.v1

Plant protoplasts, which are plant cells stripped of their cell walls through enzymatic processes, retain their totipotency, viability, and metabolic activity [12]. They are crucial for plant fundamental research and serve as invaluable tools for enhancing crop genetics [13]. Protoplasts can be isolated from various plant tissues, such as leaves, cotyledons, petals, roots, hypocotyls, suspension-cultured cells, and callus [14]. Notably, using actively growing and young tissues for isolation results in protoplasts with higher yields and improved viability [15]. Plant callus, characterised by loosely arranged, thin-walled cells with ample intercellular spaces, is particularly well-suited for protoplast isolation [16]. Among the different types of callus, embryogenic callus is preferable for enzymatic digestion due to its highly divided cells, relatively thin cell walls, and low levels of lignification and secondary metabolites like polyphenols and polysaccharides. Resulting in a higher yield and viability of protoplasts compared to non-embryogenic callus [17–20]. Additionally, protoplasts derived from embryogenic callus are more apt for transient transformation and gene function studies, laying the groundwork for plant regeneration and genetic transformation research [21]. Consequently, this study selected embryogenic callus as the source material for protoplast isolation, with systematic optimisation of the isolation conditions.

Plant protoplasts offer a versatile tool for studying gene functions, such as subcellular localisation, protein interactions, and genome editing, and can also act as intermediaries in generating stable transgenic plants [22,23]. By employing transient plasmid transfection, protoplasts can swiftly express foreign genes, facilitating rapid functional verification. Given that Agrobacterium-mediated stable transformation is expensive, time-intensive, and technically challenging, the protoplast transient transfection system presents a rapid, adaptable, and cost-effective alternative for plant molecular research [24–26]. Furthermore, protoplasts serve as efficient explants for quick gene function assays, as transfected plasmids are promptly expressed within the cells, allowing for immediate evaluation of gene activity. Subcellular localisation analysis, which identifies the intracellular distribution of gene products, is a prevalent method for functional verification [27–29]. Transient transfection systems have been successfully implemented in various plant species, including *Arabidopsis* [30,31], rice [14], maize [32], wheat [33,34], soybean [35,36], and strawberry [37], to facilitate subcellular localisation studies. Previous studies on woody plants such as *Cunninghamia lanceolata* [38], poplar [39,40], grape [41,42], citrus [27,43], walnut [23], and *Camellia oleifera* [44–46] has shown that optimising enzyme composition, digestion time, osmotic pressure, and pretreatment conditions can significantly improve protoplast yield and viability. These findings provide valuable insights for developing efficient protoplast systems in woody species.

In woody species, the thick cell walls and high concentrations of secondary metabolites, such as polyphenols and polysaccharides, render cells susceptible to damage and complicate the maintenance of viability during protoplast isolation. As a result, yields tend to be low, and a robust isolation system remains elusive. This study identified and obtained embryogenic callus of *E. ulmoides* by integrating observations of callus colour, texture, and morphology with cytological analysis, thereby offering a stable and reliable material source for protoplast preparation. The effects of enzyme composition, mannitol concentration, digestion time, and centrifugation speed were optimized to maximize protoplast yield and viability. Furthermore, the transient transformation system was optimized by investigating the effects of plasmid concentration, incubation time, and PEG4000 concentration on transformation efficiency, aiming to establish an efficient transient transformation protocol tailored for *E. ulmoides*. Collectively, this study successfully established an efficient protoplast preparation and transient transformation system based on the embryogenic callus of *E. ulmoides*, providing a valuable tool for functional genomics and genetic improvement research in this species.

2. Results

2.1. Embryogenic Callus Induction and Cytological Identification

 doi:10.20944/preprints202512.2044.v1

A two-factor, five-level full factorial L25 (5^6) experimental design was utilised to formulate media for callus induction from the hypocotyl. The results indicated that all 25 treatments successfully induced callus, with induction rates exceeding 80% in every instance. Remarkably, 12 combinations achieved induction rates above 95%, and two treatments reached a perfect 100% induction rate (Table 1). Analysis of variance revealed that both the main effects and the interaction between 6-BA and NAA concentrations on the callus induction rate were highly significant ($p < 0.001$), with 6-BA exerting the most substantial influence ($F=69.969$, $p < 0.001$). Generally, low concentrations of 6-BA, when paired with appropriate NAA levels, enhanced callus induction rates. In contrast, at high 6-BA concentrations, increasing NAA was inhibitory. The various combinations of 6-BA and NAA concentrations also significantly affected the callus's colour and texture. Based on morphological characteristics, calluses were categorised into three types: Type I—yellow, lacking obvious protrusions, loose in texture, with a water-soaked appearance (Figure 1A); Type II—light green, without obvious protrusions, dry and compact (Figure 1B); Type III—bright green, featuring spherical protrusions, dry and compact (Figure 1C).

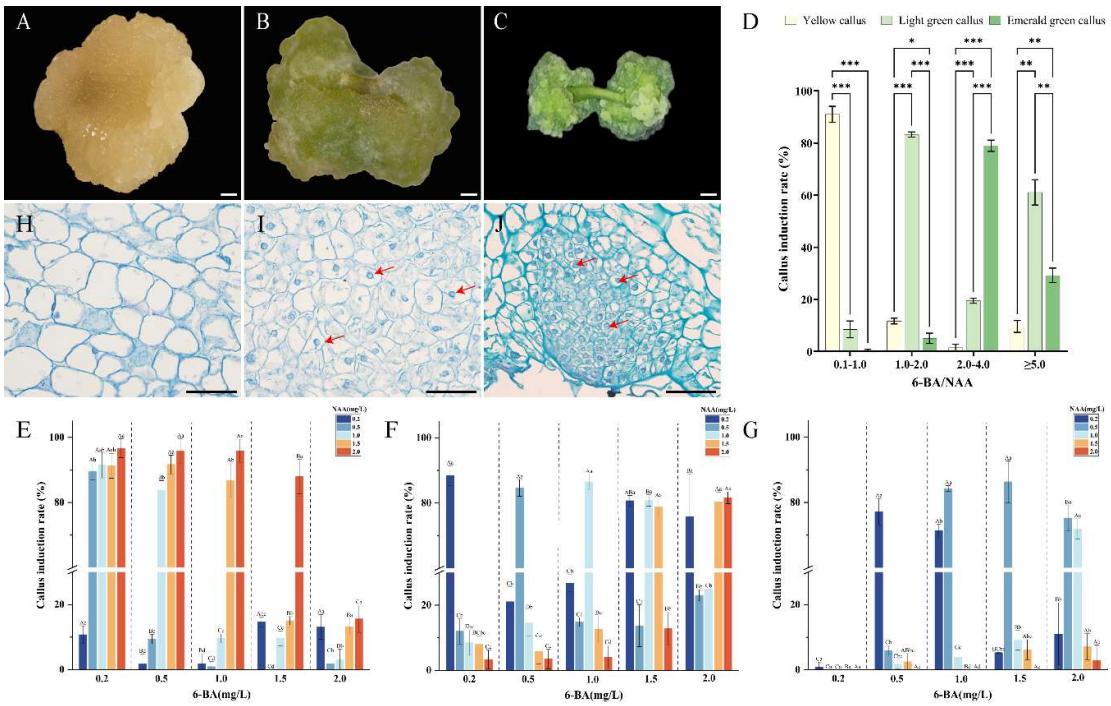

Figure 1. Effect of hormone ratios on callus type induction and morphological and cytological observations of callus in *E. ulmoides*. (A) Type I callus, scale bar = 1 mm (the same for B and C); (B) Type II callus; (C) Type III callus; (D) Induction rates of the three callus types under varying 6-BA/NAA ratios, with significant differences between means analyzed using the Least Significant Difference (LSD) test, data presented as mean ± standard error (n > 3, consistent throughout), "*", "**", "***" denote significant differences at $p < 0.05$, $p < 0.01$, and $p < 0.001$, respectively; (E, F, G) Effects of different 6-BA and NAA concentration combinations on the induction rates of Type I, II, and III callus, where different letters indicate significant differences at $p < 0.05$; (H, I, J) Cytological observations of Type I, II, and III callus under a microscope, scale bar = 100 μm, red arrows highlight the nuclei.

Table 1. Impact of various 6-BA and NAA concentration combinations on callus induction rate in *E. ulmoides*.

Treatment	6-BA (mg/L)	NAA (mg/L)	Induction rate (%)	Primary types
T1	0.2	0.2	93.33±1.44cde	Type II

 doi:10.20944/preprints202512.2044.v1

T2	0.2	0.5	97.50±0.00ab	Type I
T3	0.2	1.0	97.50±0.00ab	Type I
T4	0.2	1.5	94.17±1.44bcd	Type I
T5	0.2	2.0	100.00±0.00a	Type I
T6	0.5	0.2	95.00±0.00bc	Type III
T7	0.5	0.5	97.50±0.00ab	Type II
T8	0.5	1.0	97.50±0.00ab	Type I
T9	0.5	1.5	100.00±0.00a	Type I
T10	0.5	2.0	96.67±1.44abc	Type I
T11	1.0	0.2	93.33±1.44cde	Type III
T12	1.0	0.5	90.00±4.33efg	Type III
T13	1.0	1.0	86.67±5.77gh	Type II
T14	1.0	1.5	85.83±2.89h	Type I
T15	1.0	2.0	81.67±1.44i	Type I
T16	1.5	0.2	95.00±2.50bc	Type II
T17	1.5	0.5	97.50±0.00ab	Type III
T18	1.5	1.0	82.50±0.00i	Type II
T19	1.5	1.5	94.17±1.44bcd	Type II
T20	1.5	2.0	97.50±0.00ab	Type I
T21	2.0	0.2	88.33±3.82fgh	Type II
T22	2.0	0.5	94.17±1.44bcd	Type III
T23	2.0	1.0	80.00±0.00i	Type III
T24	2.0	1.5	93.33±1.44cde	Type II
T25	2.0	2.0	90.83±1.44def	Type II

The ratio of cytokinin to auxin is crucial in regulating callus differentiation, prompting an analysis of the 6-BA/NAA ratio's effect on callus induction rates. The findings reveal significant variations in callus induction across three types with different 6-BA/NAA ratios (Figure 1D). At a ratio of 0.1-1.0, type I callus is predominantly induced, comprising 91.1%, while type II and type III callus induction rates are lower, at 8.5% and 0.4%, respectively. When the ratio increases to 1.0-2.0, type II callus becomes predominant at 83.3%, with type I and type III at 11.6% and 5.1%, respectively. A ratio of 2.0-4.0 primarily induces type III callus (79.0%), while type II and type I are less frequent at 19.5% and 1.5%, respectively. Ratios exceeding 5.0 result in unclear callus induction directionality, with type II at 61.1%, type III at 29.2%, and type I at 9.7%. Further analysis identified optimal induction media for each callus type. For type I callus, a combination of low 6-BA (0.2-1.0 mg/L) and high NAA (1.5-2.0 mg/L) concentrations is most effective, with the highest induction rate of 96.7% achieved at 0.2 mg/L 6-BA + 2.0 mg/L NAA (Figure 1E). Type II callus induction is less dependent on absolute concentrations of 6-BA and NAA, relying more on their ratio. An optimal induction rate is achieved at a ratio of 1.0, with 0.2 mg/L 6-BA + 0.2 mg/L NAA being the most cost-effective medium, yielding an 88.4% induction rate (Figure 1F). Conversely, type III callus induction is less sensitive to 6-BA concentration but requires lower NAA levels (0.2-0.5 mg/L). Exceeding 0.5 mg/L NAA significantly reduces the induction rate, with the highest rate of 86.3% observed at 1.5 mg/L 6-BA + 0.5 mg/L NAA (Figure 1G).

To accurately identify embryonic callus for protoplast isolation, the three types of callus were processed into permanent paraffin sections for cytological observation. The analysis revealed significant differences in their cellular structures. Type I callus cells were notably large, varied in size, irregularly shaped, and loosely arranged with prominent intercellular spaces. They exhibited sparse cytoplasm, fewer nuclei, and low mitotic activity, characteristic of non-embryogenic callus (Figure

 doi:10.20944/preprints202512.2044.v1

1H). In contrast, Type II callus cells were smaller, more uniform, and regularly shaped. They were relatively compact, with clearly visible nuclei, although they had a lower nucleo-cytoplasmic ratio. Some cells demonstrated high mitotic activity and potential for differentiation (Figure 1I). Type III callus cells were small, densely packed, and orderly, with large, distinct nuclei and a high nucleo-cytoplasmic ratio, typical of embryogenic callus (Figure 1J). Consequently, hypocotyls from 15-day-old sterile *E. ulmoides* seedlings served as explants. And cultured on a medium comprising B5 + 1.5 mg/L 6-BA + 0.5 mg/L NAA + 30 g/L sucrose + 7 g/L agar, (pH =5.8), for 30 days. The resulting emerald green callus was then utilised for protoplast isolation.

2.2. Optimization of Protoplast Isolation System form Embryogenic Callus

Based on 30-day embryogenic callus, different concentrations of cellulase R-10 and macrozyme R-10 and enzymolysis time were set to evaluate their effects on protoplast yield and viability. The range analysis reveals that these three factors exert differing levels of influence on both yield and viability. Notably, the concentration of cellulase R-10 significantly affected protoplast yield, showing the highest impact ($F=746.046$, $p < 0.001$, $R=0.957$). This was followed by enzymolysis time ($F=14.426$, $p< 0.001$, $R=0.130$), with macrozyme R-10 having the least effect ($F=8.046$, $p< 0.001$, $R=0.089$). Conversely, for protoplast viability, macrozyme R-10 concentration was the most influential factor ($F=124.429$, $p< 0.001$, $R=6.88$), followed by cellulase R-10 concentration ($F=60.013$, $p< 0.001$, $R=3.82$), while enzymolysis time had the least impact ($F=0.718$, $p=0.547$, $R=0.50$).

To identify the optimal levels for protoplast isolation factors, we conducted an LSD multiple comparison analysis on yield and viability at each factor level (Figure 2). The analysis revealed that a cellulase R-10 concentration of 1.5% yielded the highest protoplast yield and viability (Figure 2A). Interestingly, as the macerozyme R-10 concentration increased, protoplast yield decreased, while viability improved (Figure 2B). Balancing both yield and viability, we determined that a macerozyme R-10 concentration of 1.0% was optimal. Prolonged enzymolysis time led to reduced yield and viability (Figure 2C), indicating that 4 h is the optimal enzymolysis duration. In addition, we performed an orthogonal experiment to comprehensively evaluate the effects of different concentrations of cellulase R-10 and macrozyme R-10, as well as enzymolysis time, on protoplast yield and viability. The findings showed a significant increase in yield up to treatment 11, followed by a sharp decline. Protoplast activity was highest in treatments 16 and 12, at 92.30% and 91.73% respectively, but treatment 11 also exhibiting a high level of 91.13%, and there was no significant difference among these treatments (Figure 2D). Consequently, we concluded that treatment 11 offers the optimal conditions for protoplast isolation, involving enzymolysis for 4 h with a combination of 1.5% cellulase R-10 and 1.0% macerozyme R-10.

 doi:10.20944/preprints202512.2044.v1

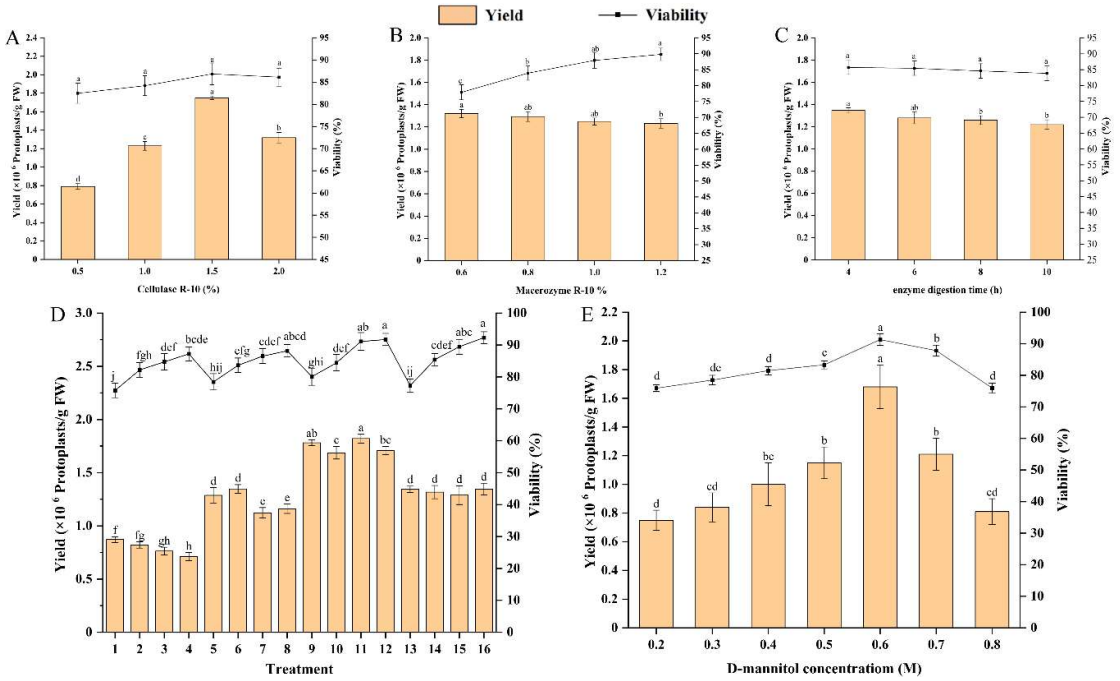

Figure 2. Optimization of protoplast isolation system derived from embryogenic callus in *E. ulmoides*. (A) Effects of cellulase R-10 concentration on protoplast yield and viability; (B) Effects of macrozyme R-10 concentration on protoplast yield and viability; (C) Effect of enzymolysis time on protoplast yield and activity; (D) The orthogonal experiment of cellulase R-10 and macerozyme R-10 concentrations as well as enzymolysis time on protoplasts yield and viability; (E) Effects of D-Mannitol concentration on protoplast yield and viability.

We examined the influence of D-mannitol concentration as an osmotic regulator on protoplast yield and viability. The concentration of D-mannitol significantly affected both yield and viability ($p<0.05$). As the D-mannitol concentration increased, protoplast yield and viability improved, peaking at 0.6 M. Beyond this concentration, both yield and viability notably declined (Figure 2E). Thus, 0.6 M D-mannitol was identified as the optimal concentration for protoplast isolation.

2.3. Optimization of Protoplast Purification Conditions

To optimise protoplast collection and eliminate impurities such as non-enzymolysis substances, cell debris, and shrunken cells, the enzymatic mixture was filtered twice through a 70 μm cell sieve and subsequently centrifuged at varying speeds. The results indicated that centrifugal speed significantly affected both the yield and viability of protoplasts ($p<0.05$), as well as their morphology (Figure 3). At 400 rpm, the protoplast yield was minimal, viability was poor, and most protoplasts clustered together (Figure 3A, B). Similarly, at 600 rpm, yield and viability remained low, with many protoplasts interconnected (Figure 3A, C). However, at 800 rpm, both yield and viability improved markedly, although the protoplasts were unevenly dispersed in the W5 solution (Figure 3A, D). The optimal results were achieved at 1000 rpm, yielding the highest protoplast count (1.82×10^6 protoplasts/g FW) and viability (92.13%), with protoplasts exhibiting complete morphology and even distribution (Figure 3A, E). Post-FDA staining, they displayed strong fluorescence and uniform staining, indicating high vitality and good physiological condition (Figure 3G, H). Conversely, increasing the speed to 1200 rpm resulted in a significant decline in yield and viability, with many protoplasts rupturing due to excessive centrifugal force (Figure 3A, F). Consequently, 1000 rpm was identified as the optimal centrifugation speed for protoplast purification.

 doi:10.20944/preprints202512.2044.v1

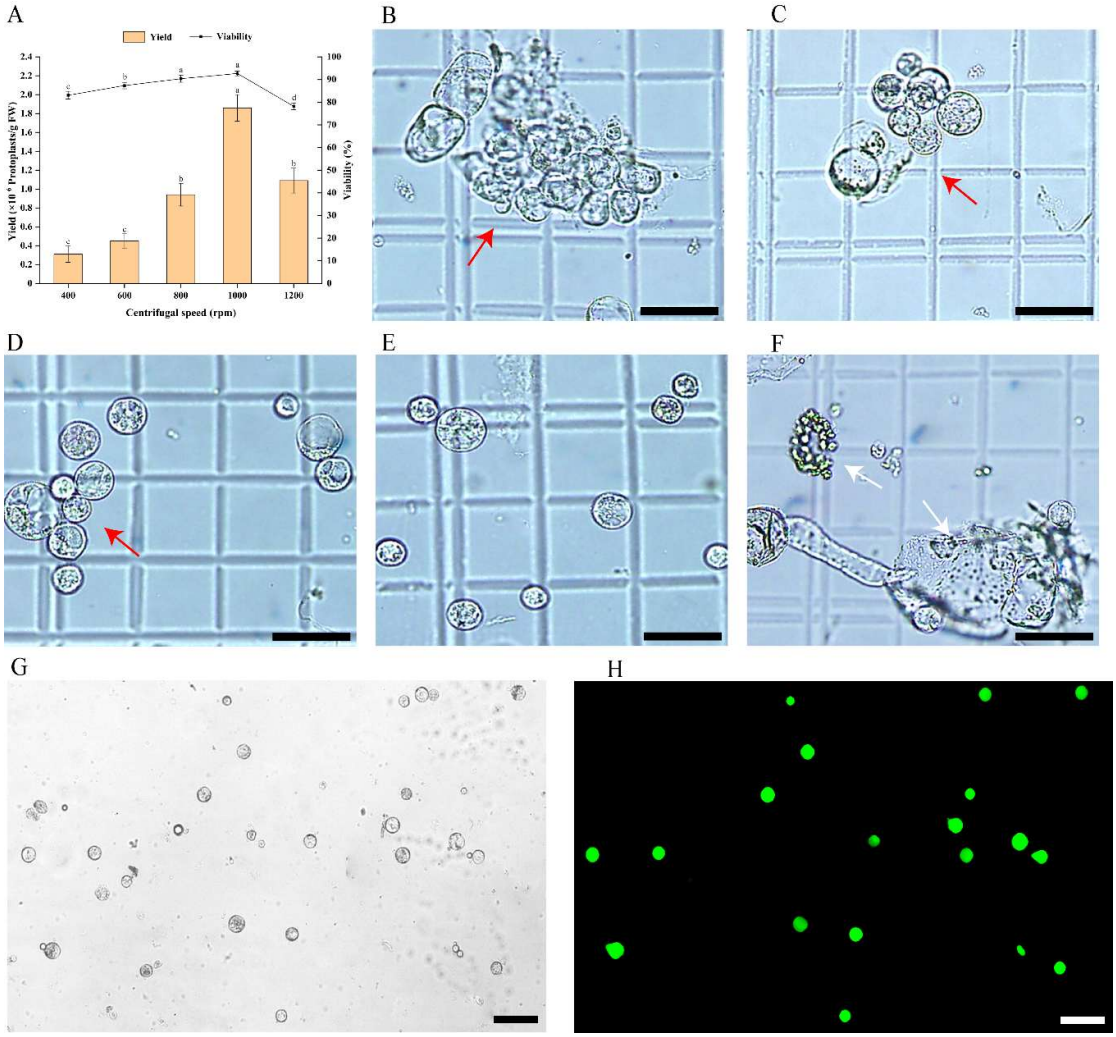

Figure 3. Effect of centrifugal speed on protoplasts purification in *E. ulmoides*. (A) Protoplast yield and viability at different centrifugal speeds; (B) Microscopic morphology of protoplasts at 400 rpm, scale bar = 50 μm (the same as C-F); (C) Microscopic morphology of protoplasts at 600 rpm; (D) Microscopic morphology of protoplasts at 800 rpm; (E) Microscopic morphology of protoplasts at 1000 rpm; (F) Microscopic morphology of protoplasts at 1200 rpm; (G, H) Observation of the morphology of protoplasts under bright field and 488 nm excitation light using a fluorescence microscope after FDA staining, scale bar = 75 μm.

In conclusion, we have established an experimental protocol for isolating and purifying protoplasts from the embryogenic callus of *E. ulmoides*, which is illustrated in a flowchart (Figure 4). According to this protocol, protoplasts with a yield of 1.82×10^6 protoplasts/g FW and a viability of 91.13% could be obtained.

 doi:10.20944/preprints202512.2044.v1

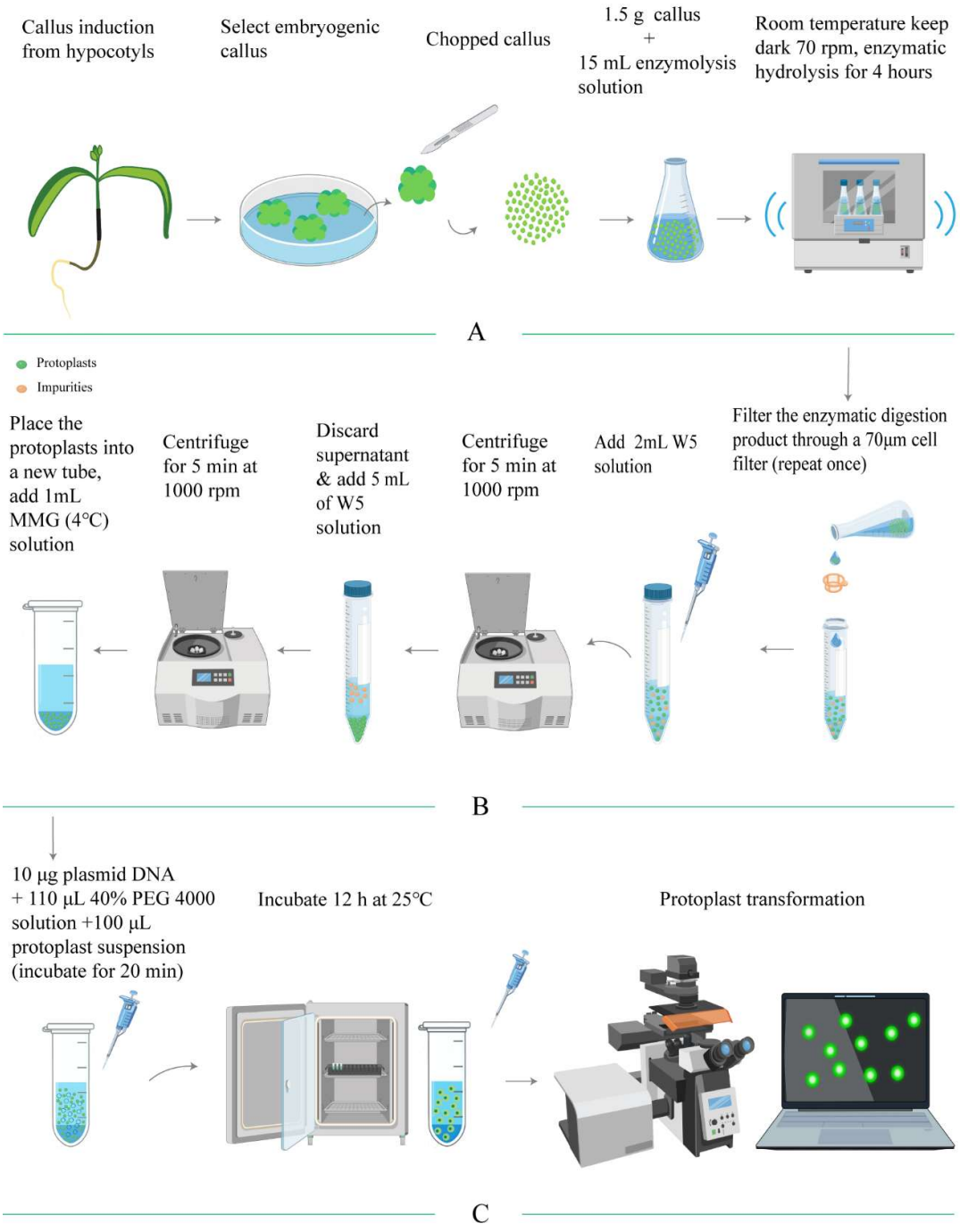

Figure 4. Illustrates the flowchart detailing the processes of protoplast isolation, purification, and transient transformation in *E. ulmoides*. (A) outlines the method for isolating protoplasts; (B) describes the purification process; (C) presents the method for transient transformation of protoplasts.

2.4. Optimization of Protoplast Transient Transformation System

To develop an efficient protoplast transient transformation system for *E. ulmoides*, we assessed the influence of plasmid concentration, PEG4000 concentration, and transformation duration on transformation efficiency. Our findings revealed that the optimal transformation efficiency (51.87%) was achieved with a plasmid concentration of 10 μg. Variations in plasmid concentration, either higher or lower, will significantly reduce the transformation rate (Figure 5A), and excessive plasmid levels caused morphological damage to protoplasts (Figure 5D, E). Furthermore, PEG4000

 doi:10.20944/preprints202512.2044.v1

concentration markedly affected the transformation rate. The optimal transformation rate of 50.63% was observed at a PEG4000 concentration of 40% (Figure 5B). Lower PEG4000 concentrations were not favourable for transient transformation, whereas higher concentrations increased protoplast rupture, thereby diminishing the transformation rate (Figure 5F). Regarding transformation time, efficiency improved with increased duration, peaking at 20 min with a rate of 53.23%. Insufficient transformation time led to inadequate contact between the plasmid and protoplasts, resulting in incomplete transformation. Conversely, extending the duration beyond 20 min caused protoplast damage, reducing the transformation rate (Figure 5C). In summary, the optimal conditions for protoplast transient transformation in *E. ulmoides* involve using 10 μg of plasmid with 40% PEG4000 for 20 min, achieving a transformation rate of 53.23%. The transformation process is illustrated in Figure 4C.

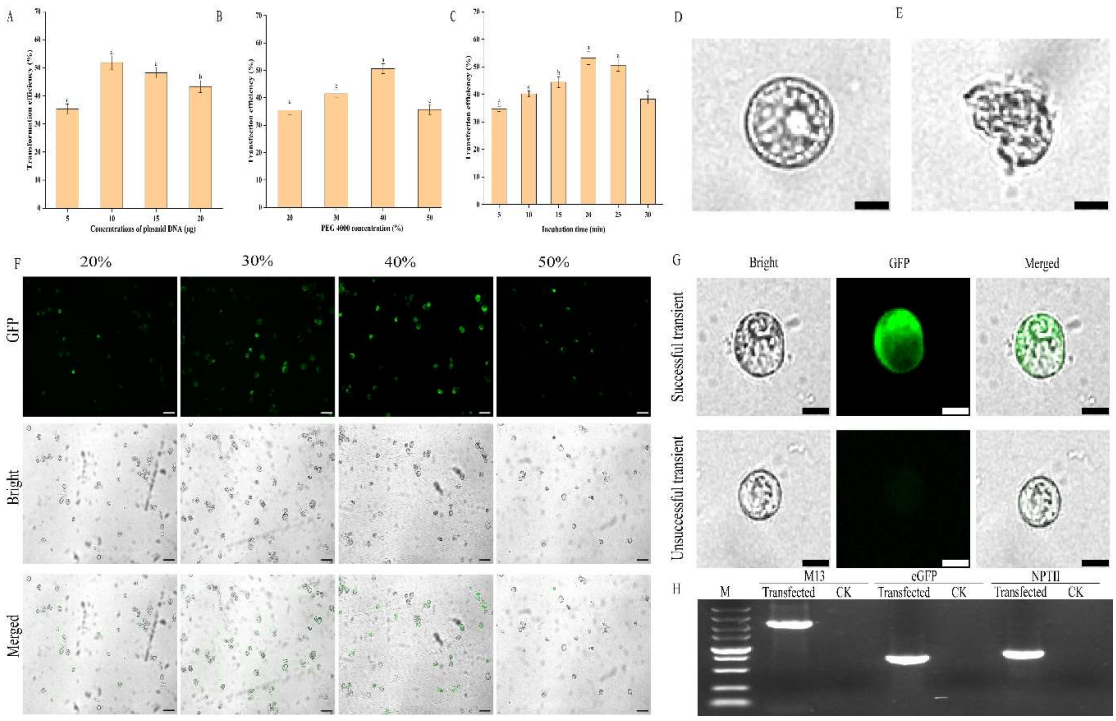

Figure 5. Effects of various factors on protoplast transformation efficiency in *E. ulmoides*. (A) The effect of plasmid concentration on transformation efficiency; (B) The effect of PEG4000 concentration on conversion efficiency; (C) The effect of incubation time on transformation efficiency; (D) Protoplasts with complete structure, scale bar=20 μm (the same for E and G); (E) Morphologically damaged protoplasts; (F) Observation of protoplast transformation under different PEG4000 concentrations by fluorescence microscope, scale bar=100 μm; (G) Observation of successfully and unsuccessfully transformed protoplasts by fluorescence microscopy; (H) Detection of the presence of pCAMBIA3301 plasmid fragment, eGFP and NPT Ⅱ in protoplasts transformed with pCAMBIA3301-*35S-eGFP* by PCR. CK represents protoplasts without transformation.

The protoplasts transformed with the pCAMBIA3301-*35S-eGFP* plasmid maintained their regular morphology and intact cell membranes when observed under a bright-field microscope. Upon excitation at 488 nm, regions expressing the *eGFP* protein emitted a distinct green fluorescence, whereas the untransformed protoplasts showed no autofluorescence (Figure 5G). Additionally, PCR analysis confirmed the presence of the pCAMBIA3301 plasmid fragment and the *eGFP* and *NPTII* genes in the transformed protoplasts, but not in the untransfected ones (Figure 5H). These results indicated that pCAMBIA3301-*35S-eGFP* plasmid had been successfully introduced into protoplasts, resulting in transient expression.

 doi:10.20944/preprints202512.2044.v1

3. Discussion

E. ulmoides is a valuable woody plant with notable medicinal and industrial applications [47]. Due to its slow growth, research on the regulation and production of its natural metabolites, functional genes, and molecular breeding primarily relies on plant tissue culture techniques [48,49]. Since 1980, numerous studies on tissue culture of *E. ulmoides* have been reported, investigating various parts such as hypocotyls, cotyledons, leaves, bud-bearing stem segments, and both mature and immature embryos [50,51]. Currently, the exploration and validation of functional genes in *E. ulmoides* predominantly utilise *Agrobacterium*-mediated transformation with hypocotyls as explants. However, the incomplete transgenic regeneration system significantly limits the application of functional genes and molecular breeding research [52,53]. Plant protoplasts are living cells without cell walls, can directly absorb exogenous DNA and undergo somatic hybridisation, making them widely used for genetic modification and improvement in plants [54]. Embryogenic callus is generally regarded as an excellent material for protoplast isolation and culture, forming a crucial foundation for developing an efficient protoplast isolation system [46]. Consequently, this study established a system for inducing embryogenic callus from hypocotyls, isolating protoplasts, and implementing PEG-mediated transient transformation in *E. ulmoides*. This provides a reliable platform for the rapid analysis of gene function and genetic manipulation.

Previous research primarily utilised MS medium combined with 6-BA and NAA to induce callus formation and proliferation in *E. ulmoides* [50,51]. Wang et al. [55] discovered that B5 medium significantly outperformed MS medium concerning callus growth, average budding rate, and positive bud ratio post-transformation. Therefore, this study employed hypocotyls as explants to examine the effects of varying concentrations of 6-BA and NAA in solid B5 medium on the callus type and embryogenic potential of *E. ulmoides*. The results showed that all 25 media combinations produced three distinct callus states, differing in colour, shape, and texture (Figure 1 A–C). Traditionally, callus embryogenicity was assessed solely based on external characteristics such as colour, shape, and texture [56,57], which posed observational challenges. To address this, we conducted cytological observations using the paraffin section technique. In this study, both Type II and Type III callus exhibited clearly observable nuclei, indicative of embryogenic cells. However, the globular embryos formed in Type III callus were characteristic of embryogenic callus, suggesting superior potential for genetic transformation and redifferentiation. The external morphology of Type III callus was described as “dry, dense, emerald-green spherical protrusions”, aligning with descriptions in existing literature [58,59]. In this study, the average callus induction rates for 12 culture media exceeded 95%. The concentration ratio of 6-BA to NAA significantly influenced callus type. When the ratio ranged from 2.0 to 4.0, the proportion of Type III callus was highest. Conversely, at ratios ≥ 5.0, the proportion of embryogenic callus decreased, and direct induction of adventitious buds was observed. Considering the analysis of Type III callus proportions, the optimal callus induction medium for *E. ulmoides* hypocotyls was determined to be B5 + 1.5 mg/L 6-BA + 0.5 mg/L NAA.

High-quality protoplasts are essential for transformation and functional gene analysis [54]. The plant cell wall primarily comprises cellulose and pectin, with compositions varying across species and even within different organs of the same species [60]. Therefore, the enzymatic method for protoplast isolation must be tailored to the specific cell wall components of the plant material in question [23]. The choice and concentration of cell wall-degrading enzymes, along with the enzymolysis duration, are pivotal in optimising protoplast yield and viability [61]. In previous research, a complex enzyme mix (2.5% cellulase R-10, 0.6% macerozyme R-10, 2.5% pectinase, and 0.5% hemicellulase) yielded 1.13×10^6 protoplasts/g FW from young *E. ulmoides* stems [62]. However, our study demonstrates that a simpler combination of 1.5% cellulase R-10 and 1.0% macerozyme R-10 achieves a higher yield of 1.82×10^6 protoplasts/g FW. This could be attributed to the more intricate cell wall structure of young *E. ulmoides* stems compared to embryogenic callus. The results suggest that callus is a more suitable material for protoplast isolation, aligning with Russell’s results [63]. Numerous studies indicate that increasing enzyme concentration boosts protoplast yield but

 doi:10.20944/preprints202512.2044.v1

diminishes viability [62,64]. Interestingly, our research found that the cellulase R-10 concentration had no significant effect on protoplast viability, but higher macerozyme R-10 concentrations reduce yield but enhance viability. This may occur because increased macerozyme R-10 concentrations improve cell wall degradation efficiency but also stress cells, causing fragile ones to rupture, leaving behind more resilient protoplasts. Enzymolysis duration varies significantly among plant species and tissues. For instance, isolating protoplasts requires 18 h from sweet cherry pulp [65], 15 h from strawberry leaves [25], 10 h from young *E. ulmoides* stems [62]. In contrast, our study requires only 4 h for embryogenic callus of *E. ulmoides*, similar to the 3-4 h needed for *C. lanceolata* callus [66]. This efficiency is likely due to the thinner cell walls of callus, which degrade more readily. A shorter enzymolysis period generally prevents protoplast degradation, facilitating their subsequent use [66]. The protoplast isolation system developed in this study, with its brief enzymolysis time, ensures the protoplasts remain in a good physiological state, providing a solid foundation for further studies on gene function, protein subcellular localisation, and protein interaction.

When protoplasts are devoid of a cell wall, they can contract, expand, or even rupture due to their inability to maintain isobaric conditions with the external environment [62]. To counteract this, an appropriate concentration of D-mannitol is typically added to the enzymatic solution to balance the osmotic pressure. Researches have indicated that a 0.4 M concentration of D-mannitol is optimal for isolating protoplasts in various plants, including poplar, *C. lanceolata*, and Camellia sinensis [67]. However, both this study and Hu et al. [62] identified that a 0.6 M concentration is necessary for *E. ulmoides*. This higher requirement is likely due to the elevated solute concentration in *E. ulmoides* cells, which contain numerous macromolecular substances like *Eu*-rubber, necessitating a greater concentration of D-mannitol to achieve osmotic balance.

PEG4000 facilitates the uptake of exogenous DNA into protoplasts by altering the physicochemical properties of the cell membrane surface and enhancing membrane permeability. However, its transformation efficiency is influenced by concentration, plasmid dosage, and transformation duration [12,26]. Our study identified that a 40% concentration of PEG4000 optimally supports transformation. Both excessive and insufficient concentrations markedly decrease efficiency, consistent with findings in other plant species [68]. This suggests that approximately 40% PEG4000 strikes an optimal balance between high membrane permeability and low cytotoxicity across various plants, including *E. ulmoides*. The results of this study indicate that a transformation rate of 53.23% can be achieved with just 10 μg plasmid for 20 min. This plasmid quantity is notably lower than that required for other species, such as *S. spontaneum* [13], *Camellia yubsienensis* [69], *P. aegyptiaca* [7]. Additionally, both the plasmid dosage and transformation rate surpass those observed in the transient transformation of protoplasts isolated from young stems [62]. This enhanced efficiency may be attributed to the higher membrane permeability of protoplasts derived from *E. ulmoides* embryogenic callus at 40% PEG4000. These results underscore the advantages of the protoplasts obtained through this experimental approach for further research in *E. ulmoides*.

4. Materials and Methods

4.1. Plant Materials and Culture Conditions

Mature seeds were removed from their shells and soaked in water for 8 h. They were then washed with a detergent containing a surfactant and thoroughly rinsed under running tap water for 30 min to ensure all residues were eliminated. Subsequently, the seeds were placed on a sterilised ultra-clean table, soaked in 75% (v/v) ethanol for 30 s, and rinsed 1-2 times with sterile water. Following this, they were immersed in 10% NaClO (v/v) for 20 min and rinsed 4-5 times with sterile water. The sterilised seeds were trimmed at both ends and inoculated onto Murashige and Skoog (MS) [70] medium containing 10 mg/L GA_3, with a pH of 5.8 ± 0.2. The cultures were maintained at a temperature of 24 ± 2 ℃ under a 16 h/8 h light-dark cycle. After 15 days, the sterile seedlings of *E. ulmoides* reached a height of 5-8 cm, with hypocotyls measuring 3-5 cm.

 doi:10.20944/preprints202512.2044.v1

4.2. Callus Induction and Embryogenic Callus Identification

The hypocotyls were sliced into 5-8 mm and inoculated onto B5 medium with varying concentrations of 6-BA and NAA. A two-factor, five-level full factorial experimental design (L25(5^6)) was employed, 6-BA and NAA concentrations set at 0.2 mg/L, 0.5 mg/L, 1.0 mg/L, 1.5 mg/L, and 2.0 mg/L, respectively, resulting in 25 distinct treatment combinations (Table1). Each treatment included 30 explants and was replicated three times. The cultures were maintained under these conditions until callus formation was observed.

The paraffin sectioning method, adapted from Li's approach [71], was utilised to distinguish between embryogenic and non-embryogenic callus. In brief, the callus was fixed in a 50% FAA solution for 24 h, dehydrated through a gradient ethanol series, embedded in paraffin, and then sliced into 8 μm-thick sections, stained with safranin-fast green, sealed with neutral gum, and observed under an optical microscope.

4.3. Protoplast Isolation and Purification

The isolation and purification of protoplasts were optimized according to the protocols of Yang [40] and He [46]. Briefly, 1.5 g of embryogenic callus was sliced into 1-2 mm particles and swiftly transferred into 15 mL of an enzyme solution which containing 0.1% BSA, 10 mM $CaCl_2$, 0.1% MES, 0.6 M mannitol and varying concentrations of cellulase R-10 and macerozyme R-10 (both from YAKSIOR, Japan). The mixture was then subjected to enzymatic treatment at 25 °C and 70 rpm in darkness for 4-10 h to dissolve the cell wall and release the protoplasts. To determine the optimal conditions for protoplast isolation, A three-factor and four-level orthogonal design (L16(4^3)) was employed. This design examined the concentrations of cellulase R-10 (0.5, 1.0, 1.5, 2.0%) and macerozyme R-10 (0.6, 0.8, 1.0, 1.2%), alongside the enzymatic hydrolysis duration (4, 6, 8, 10 h), resulting in sixteen distinct treatments. Following the identification of the optimal enzyme concentrations and digestion time, various D-mannitol concentrations (0.2, 0.3, 0.4, 0.5, 0.6, 0.7, 0.8 M) were tested to ensure the ideal osmotic pressure was maintained.

For purification, the hydrolysate was filtered twice through a 70 μm cell strainer to remove larger tissue. Subsequently, centrifugation was conducted at varying speeds (400, 600, 800, 1000, and 1200 rpm) for 5 min at room temperature to investigate the enrichment effect of centrifugal force on protoplasts. Then, the obtained protoplasts were resuspended in 5 mL of W5 solution (comprising 154 mM NaCl, 125 mM $CaCl_2$, 5 mM KCl, 5 mM glucose, 2 mM MES) and washed three times. Finally, the protoplasts were resuspended in 1 mL of MMG solution (containing 15 mM $MgCl_2$, 4 mM MES, 0.5 M mannitol) and incubated on ice for 30 min to assess the yield and viability of the protoplasts and perform transient transformation.

4.4. Protoplast Yield and Viability Assessment

The yield of protoplasts was assessed using a hemocytometer under an optical microscope (Olympus, Tokyo, Japan, BX61). Protoplasts were stained with 0.1% (w/v) fluorescein diacetate (FDA) in darkness for 5 min, after which their viability was examined using a fluorescence microscope (Zeiss, Oberkochen, Germany, Axio Imager M2). Protoplasts exhibiting green fluorescence were deemed viable. The calculations for protoplast yield and viability were as follows: Protoplast yield (protoplasts/g FW) = total number of protoplasts obtained / fresh weight of calls; Protoplast viability (%) = (number of the fluorescent protoplasts/ total number of protoplasts) ×100%. Each treatment was conducted in triplicate.

4.5. Protoplast Transformation

Polyethylene glycol (PEG)-mediated protoplast transfection was carried out as described by Zhang [37] and Yang [40] with slight modifications. In brief, freshly isolated protoplasts were suspended in MMG solution (15 mM $MgCl_2$, 0.6 M mannitol, 4 mM MES, pH = 5.7) to reach a final concentration of 1 × 10^5 protoplasts/mL. The purified pCAMBIA3301-*35S-eGFP* plasmid was

 doi:10.20944/preprints202512.2044.v1

introduced into a 2 mL round-bottom tube containing 110 μL of PEG buffer (containing 0.6 M mannitol and 0.1 M $CaCl_2$) and 100 μL of the protoplast suspension, then gently mixed. After infection for various durations at 25℃ in the dark, added 420 μL of W5 solution to terminate the transformation. Then, the mixture was centrifuged at 1000 rpm for 5 min, discarded supernatant, and washed the protoplasts twice with W5 solution.

To optimise transformation conditions, transient transformation experiments were conducted using varying concentrations of plasmid DNA (5 μg, 10 μg, 15 μg, 20 μg) with 40% PEG4000 and an incubation period of 20 min. Additionally, different PEG4000 concentrations (20%, 30%, 40%, 50%) were tested, maintaining a 20-min incubation and using 10 μg of plasmid. For the combination of 40% PEG4000 and 10 μg plasmid DNA, incubation times were varied at 5, 10, 15, 20, 25, and 30 min. The transformed protoplasts were cultured in darkness at 25 °C for 12 h before being examined under a fluorescence microscope. GFP expression in the transfected protoplasts was observed using a fluorescence microscope with an excitation wavelength of 488 nm. Transformation efficiency was calculated using the formula: Transformation efficiency (%) = (number of fluorescent protoplasts / total number of protoplasts) × 100%. Each experiment was conducted three times, observing five fields per replicate.

4.6. Detection of Transfected Protoplasts by PCR

Total genomic DNA from transfected and untransfected (control) protoplasts was extracted using the DNAsecure Plant Kit (TIANGEN, Beijing, China). M13 universal primers and *eGFP* and *NPTII* specific primers were used to detect the presence of pCAMBIA3301-*35S-eGFP* in the transfected protoplasts but not in the untransfected ones (Table 2).The PCR procedure was pre-denatured at 94 ℃ for 3 min; 35 cycles of denatured at 94 ℃ for 30 s, annealed at 58 ℃ for 30 s, extended at 72 ℃ for 1 min; and extended at 72 ℃ for 5 min. Subsequently, PCR products were analyzed by 1% (w/v) agarose gel electrophoresis.

Table 2. Primer information for detecting the pCAMBIA3301-*35S-eGFP* plasmid [64].

	Forward (5′-3′)	**Reverse (5′-3′)**	**Tm (℃)**
M13	CAGGAAACAGCTATGAC	GTAAAACGACGGCCAGT	58
eGFP	GGTACCCGGGGATCCTCT	GAAAGCTCTGCAGGAATTCGATT	58
NPTI *I*	AACTCACGTTAAGGGATTTTGGTCAT	CTCTTGGGGTATCTTTAAATACTGTAGAAAAGAGGA	58

4.7. Data Analysis

The statistical analysis was conducted using IBM SPSS Statistics Version 21.0 (SPSS Inc., Chicago, IL, USA). A one-way analysis of variance (ANOVA) followed by a post hoc least significant difference (LSD) test was employed. For multi-factor orthogonal experiments, the LSD test was similarly applied. Range analysis was conducted on the orthogonal test results, with the range value (R) indicating the magnitude of each factor's effect on the experimental outcomes. Data are presented as mean ± standard deviation from three independent experiments. A p-value of less than 0.05 was considered statistically significant.

5. Conclusions

In this study, we established an efficient and reproducible system for embryogenic callus induction, protoplast isolation, and PEG-mediated transient transformation in *E. ulmoides*. The optimal conditions yielded high-quality protoplasts with excellent viability and achieved a

 doi:10.20944/preprints202512.2044.v1

transformation efficiency exceeding 53%. This system provides a powerful platform for rapid gene function analysis, genome editing, and molecular breeding in *E. ulmoides*, thereby advancing genetic and biotechnological research on this valuable tree species.

Author Contributions: H.Z. was responsible for designing and conducting the experiments, analysing the data, and drafting the manuscript. Z.Z. contributed to the experiments and reviewed the manuscript. J.Z. focused on data analysis. H.K. also participated in performing the experiments. Both M.Y. and H.Z. were involved in data analysis, while L.W. handled data analysis and image processing. J.Y. managed the project, secured funding, designed the experiments, and reviewed the manuscript. J.Z. was involved in securing funding and reviewing the manuscript. All authors have read and approved the final version of the manuscript.

Funding: This research received financial support from the National Natural Science Foundation of China (Grant No. 32001913 and Grant No. 32360397) and the Shihezi University Young Innovative Talents Program (No. CXBJ202101).

Data Availability Statement: All data are included in the present study.

Acknowledgments: The author extends heartfelt gratitude to Xiaojian Zeng for her meticulous guidance and patient assistance in experimental design and key technical operations. Appreciation is also due to Ke Meng for his collaborative support throughout the experiment. Special thanks to Dr. Xiaolei Cao for providing the pCAMBIA3301-35S-eGFP plasmid. The author is also grateful to Professor Zhaoqun Yao for his valuable suggestions for this research. During the preparation of this manuscript, Sci Draw and Bio GDP were utilised for creating scientific research vector graphics.

Conflicts of Interest: The authors declare no conflicts of interest.

References

1. Dong, C.; Zhang, Z.; Shao, Q.; Yao, T.; Hu, H.; Huang, J.; Liang, Z.; Han, Y. Deciphering the effects of genetic characteristics and environmental factors on pharmacological active ingredients of *Eucommia ulmoides*. *Ind. Crop Prod.* **2022**, *175*, doi:10.1016/j.indcrop.2021.114293.
2. Du, Q.; Song, K.; Wang, L.; Du, L.; Du, H.; Li, B.; Li, H.; Yang, L.; Wang, Y.; Liu, P. Integrated transcriptomics and metabolomics analysis promotes the understanding of adventitious root formation in *Eucommia ulmoides* Oliver. *Plants* **2024**, *13*, doi:10.3390/plants13010136.
3. Wang, C.; Gong, H.; Feng, M.; Tian, C. Phenotypic variation in leaf, fruit and seed traits in natural populations of *Eucommia ulmoides*, a relict Chinese endemic tree. *Forests* **2023**, *14*, doi:10.3390/f14030462.
4. Kong, F.; Zeng, Q.; Li, Y.; Ding, Y.; Xue, D.; Guo, X. Improving antioxidative and antiproliferative properties through the release of bioactive compounds from *Eucommia ulmoides* Oliver bark by steam explosion. *Front. Nutr.* **2022**, *9*, doi:10.3389/fnut.2022.916609.
5. Pan, Y.; Ming, K.; Guo, D.; Liu, X.; Deng, C.; Chi, Q.; Liu, X.; Wang, C.; Xu, K. Non-targeted metabolomics and explainable artificial intelligence: Effects of processing and color on coniferyl aldehyde levels in *Eucommiae* cortex. *Food Chem.* **2024**, *460*, doi:10.1016/j.foodchem.2024.140564.
6. Sun, Y.; Guo, J. Research progress on breeding of *Eucommia ulmoide*s and application prospect. *J. Zhejiang For. Sci. Technol*. **2024**, 44, 111–118.
7. Han, Z.; Wang, Q.; Li, Y.; Liao, X.; Sun, R.; Xie, M. Extracting *Eucommia ulmoides* gum from *Eucommia ulmoides* Oliver and exploiting the residue as sustainable filler. *Ind. Crop Prod.* **2024**, *222*, doi:10.1016/j.indcrop.2024.119585.
8. Duan, C.; Han, X.; Chang, Y.; Xu, J.; Yue, G.; Zhang, Y.; Fu, Y. A novel ternary deep eutectic solvent pretreatment for the efficient separation and conversion of high-quality gutta-percha, value-added lignin and monosaccharide from *Eucommia ulmoides* seed shells. *Bioresour. Technol.* **2023**, *370*, doi:10.1016/j.biortech.2022.128570.
9. Bao, L.; Sun, Y.; Wang, J.; Li, W.; Liu, J.; Li, T.; Liu, Z. A review of "plant gold" *Eucommia ulmoides* Oliv.: A medicinal and food homologous plant with economic value and prospect. *Heliyon* **2024**, *10*, doi:10.1016/j.heliyon.2024.e24851.

 doi:10.20944/preprints202512.2044.v1

10. Wang, Q.; Hu, F.; Yao, Z.; Zhao, X.; Chu, G.; Ye, J. Comprehensive genomic characterisation of the NAC transcription factor family and its response to drought stress in *Eucommia ulmoides*. *PeerJ* **2023**, *11*, doi:10.7717/peerj.16298.
11. Zuo, Y.; Li, B.; Guan, S.; Jia, J.; Xu, X.; Zhang, Z.; Lu, Z.; Li, X.; Pang, X. *EuRBG10* involved in indole alkaloids biosynthesis in *Eucommia ulmoides* induced by drought and salt stresses. *J. Plant Physiol.* **2022**, *278*, doi:10.1016/j.jplph.2022.153813.
12. Du, J.; Zhang, H.; Li, W.; Li, X.; Wang, Z.; Zhang, Y.; Xiong, A.; Li, M. Optimization of protoplast preparation system from leaves and establishment of a transient transformation system in *Apium graveolens*. *Agronomy* **2023**, *13*, doi:10.3390/agronomy13082154.
13. Jaganathan, D.; Ramasamy, K.; Sellamuthu, G.; Jayabalan, S.; Venkataraman, G. CRISPR for crop improvement: an update review. *Front. Plant Sci.* **2018**, *9*, doi:10.3389/fpls.2018.00985.
14. Poddar, S.; Tanaka, J.; Cate, J.H.D.; Staskawicz, B.; Cho, M.J. Efficient isolation of protoplasts from rice calli with pause points and its application in transient gene expression and genome editing assays. *Plant Methods* **2020**, *16*, doi:10.1186/s13007-020-00692-4.
15. Kang, H.H.; Naing, A.H.; Kim, C.K. Protoplast isolation and shoot regeneration from protoplast-derived callus of *Petunia hybrida* Cv. Mirage Rose. *Biology* **2020**, *9*, doi:10.3390/biology9080228.
16. Zhu N.; L. J.; Zhang X.; Dong J. Preparation and vitality detection of protoplast in *Salvia miltiorrhiza* Bunge. *Chin. J. Biotechnol.* **2014**, *30*, 1612-1621.
17. Blanc, G.; Lardet, L.; Martin, A.; Jacob, J.L.; Carron, M.P. Differential carbohydrate metabolism conducts morphogenesis in embryogenic callus of *Hevea brasiliensis* (Müll. Arg.). *J. Exp. Bot.* 2002, 53, 1453-1462. doi:10.1093/jexbot/53.373.1453.
18. Baskaran, P.; Kumari, A.; Naidoo, D.; Van Staden, J. In vitro propagation and ultrastructural studies of somatic embryogenesis of *Ledebouria ovatifolia*. In Vitro *Cell. Dev. Pl.* **2016**, *52*, 283-292, doi:10.1007/s11627-016-9762-9.
19. Neves, N.; Segura-Nieto, M.; Blanco, M.A.; Sánchez, M.; González, A.; González, J.L.; Castillo, R. Biochemical characterization of embryogenic and non-embryogenic calluses of sugarcane. In Vitro *Cell. Dev. Pl.* **2003**, *39*, 343-345, doi:10.1079/ivp2002391.
20. Mudiam, M.K.R.; Ng, T.L.M.; Karim, R.; Tan, Y.S.; Teh, H.F.; Danial, A.D.; Ho, L.S.; Khalid, N.; Appleton, D.R.; Harikrishna, J.A. Amino acid and secondary metabolite production in embryogenic and non-embryogenic callus of fingerroot ginger *(Boesenbergia rotunda)*. *Plos One* **2016**, *11*, doi:10.1371/journal.pone.0156714.
21. Huang, X.; Wang, Y.; Xu, J.; Wang, N. Development of multiplex genome editing toolkits for citrus with high efficacy in biallelic and homozygous mutations. *Plant Mol. Biol.* **2020**, *104*, 297-307, doi:10.1007/s11103-020-01043-6.
22. Omar, A.A.; Murata, M.M.; El-Shamy, H.A.; Graham, J.H.; Grosser, J.W. Enhanced resistance to citrus canker in transgenic mandarin expressing Xa21 from rice. *Transgenic Res.* **2018**, *27*, 179-191, doi:10.1007/s11248-018-0065-2.
23. Gao, Y.; Tang, T.; Cao, W.; Ali, M.; Zhou, Q.; Zhu, D.; Ma, X.; Cai, Y.; Zhang, Q.; Wang, Z.; et al. Protoplast transient transformation facilitates subcellular localization and functional analysis of walnut proteins. *Plant Physiol.* **2025**, *197*, doi:10.1093/plphys/kiae627.
24. Wang, Q.; Zhang, M.; Han, M.; Rong, J.; Peng, W.; Wang, Y.; Zhao, Y.; Lei, X.; Zhang, J.; Wang, Y. Development of a transient expression system for *Panax ginseng* based on protoplast isolation from its embryoids. *Hortic. Plant J.* **2025**, *11*, 459-462, doi:10.1016/j.hpj.2024.06.006.
25. Gou, Y.; Li, Y.; Bi, P.; Wang, D.; Ma, Y.; Hu, Y.; Zhou, H.; Wen, Y.; Feng, J. Optimization of the protoplast transient expression system for gene functional studies in strawberry *(Fragaria vesca)*. *Plant Cell, Tiss. Org.* **2020**, *141*, 41-53, doi:10.1007/s11240-020-01765-x.
26. Chen, K.; Chen, J.; Pi, X.; Huang, L.; Li, N. Isolation, purification, and application of protoplasts and transient expression systems in plants. *Int. J. Mol. Sci.* **2023**, *24*, doi:10.3390/ijms242316892.
27. Yang, W.; Ren, J.; Liu, W.; Liu, D.; Xie, K.; Zhang, F.; Wang, P.; Guo, W.; Wu, X. An efficient transient gene expression system for protein subcellular localization assay and genome editing in citrus protoplasts. *Hortic. Plant J.* **2023**, *9*, 425-436, doi:10.1016/j.hpj.2022.06.006.

 doi:10.20944/preprints202512.2044.v1

28. Yang, P.; Sun, Y.; Sun, X.; Li, Y.; Wang, L. Optimization of preparation and transformation of protoplasts from *Populus simonii* × *P. nigra* leaves and subcellular localization of the major latex protein 328 (MLP328). *Plant Methods* **2024**, *20*, doi:10.1186/s13007-023-01128-5.
29. Jin, J.; Gui, S.; Li, Q.; Wang, Y.; Zhang, H.; Zhu, Z.; Chen, H.; Sun, Y.; Zou, Y.; Huang, X.; et al. The transcription factor $GATA_{10}$ regulates fertility conversion of a two-line hybrid *tms5* mutant rice via the modulation of Ub_{L40} expression. *J. Integr. Plant Biol.* **2019**, *62*, 1034-1056, doi:10.1111/jipb.12871.
30. Jung, H.; Yan, J.; Zhai, Z.; Vatamaniuk, O.K. Gene functional analysis using protoplast transient assays. *Methods Mol. Biol.* 2015; 1284, 433-452, doi: 10.1007/978-1-4939-2444-8-22.
31. Razzak, M.A.; Lee, J.; Lee, D.W.; Kim, J.H.; Yoon, H.S.; Hwang, I. Expression of seven carbonic anhydrases in red alga *Gracilariopsis chorda* and their subcellular localization in a heterologous system, *Arabidopsis thaliana*. *Plant Cell Rep.* **2018**, *38*, 147-159, doi:10.1007/s00299-018-2356-8.
32. Zhang, X.; Xiao, K.; Li, S.; Li, J.; Huang, J.; Chen, R.; Pang, S.; Zhou, X. Genome-wide analysis of the *NAAT*, *DMAS*, *TOM*, and *ENA* gene families in maize suggests their roles in mediating iron homeostasis. *BMC Plant Biol.* **2022**, *22*, doi:10.1186/s12870-021-03422-7.
33. Han, S.; Qu, G.; Li, X.; Zhang, F. Highly efficient endosperm and pericarp protoplast preparation system for transient transformation of endosperm-related genes in wheat. *Plant Cell, Tiss. Org.* **2023**, *155*, 165-174, doi:10.1007/s11240-023-02561-z.
34. Qin, D.; Liu, G.; Liu, R.; Wang, C.; Xu, F.; Xu, Q.; Ling, Y.; Dong, G.; Peng, Y.; Ge, S.; et al. Positional cloning identified *HvTUBULIN8* as the candidate gene for round lateral spikelet (RLS) in barley *(Hordeum vulgare L.)*. *Theor. Appl. Genet.* **2023**, *136*, doi:10.1007/s00122-023-04272-7.
35. Hanzawa, Y.; Wu, F. A simple method for isolation of soybean protoplasts and application to transient gene expression analyses. *J. o. V. E.* **2018**, 25, doi:10.3791/57258.
36. Kim, K.; Shin, J.; Lee, J.D.; Kim, W.C. Establishment of efficient hypocotyl-derived protoplast isolation and its application in soybean *(Glycine max* [L.] Merr.*)*. *Front. Plant Sci.* **2025**, *16*, doi:10.3389/fpls.2025.1587927.
37. Zhang, X.; Peng, R.; Tian, X.; Guo, Y.; Li, X.; Liu, X.; Xie, Y.; Li, M.; Xia, H.; Liang, D. Establishment of protoplasts isolation and transient transformation system for kiwifruit. *Sci. Hortic.* **2024**, *329*, doi:10.1016/j.scienta.2024.113034.
38. Hong, K.; Chen, Z.; Radani, Y.; Zheng, R.; Zheng, X.; Li, Y.; Chen, J.; Yang, L. Establishment of PEG-mediated transient gene expression in protoplasts isolated from the callus of *Cunninghamia lanceolata*. *Forests* **2023**, *14*, doi:10.3390/f14061168.
39. Yang, Y.; Lee, J.H.; Poindexter, M.R.; Shao, Y.; Liu, W.; Lenaghan, S.C.; Ahkami, A.H.; Blumwald, E.; Stewart, C.N. Rational design and testing of abiotic stress-inducible synthetic promoters from poplar *cis*-regulatory elements. *Plant Biotechnol. J.* **2021**, *19*, 1354-1369, doi:10.1111/pbi.13550.
40. Yang, C.; Yu, R.; Li, J.; Wang, K.; Liu, G. Preparation of leaf protoplasts from Populus *(Populus* × *xiaohei* T. S. Hwang et Liang*)* and establishment of transient expression system. *J. Plant Physiol.* **2023**, *291*, doi:10.1016/j.jplph.2023.154122.
41. Tricoli, D.M.; Debernardi, J.M. An efficient protoplast-based genome editing protocol for *Vitis* species. *Hortic. Res.* **2024**, *11*, doi:10.1093/hr/uhad266.
42. Zhao, F.; Li, Y.; Hu, Y.; Gao, Y.; Zang, X.; Ding, Q.; Wang, Y.; Wen, Y. A highly efficient grapevine mesophyll protoplast system for transient gene expression and the study of disease resistance proteins. *Plant Cell, Tiss. Org.* **2015**, *125*, 43-57, doi:10.1007/s11240-015-0928-7.
43. Cai, X.; Fu, J.; Guo, W. Mitochondrial genome of callus protoplast has a role in mesophyll protoplast regeneration in *Citrus*: evidence from transgenic GFP somatic homo-fusion. *Hortic. Plant J.* **2017**, *3*, 177-182, doi:10.1016/j.hpj.2017.10.001.
44. Lin, Z.; Huang, L.; Yu, P.; Chen, J.; Du, S.; Qin, G.; Zhang, L.; Li, N.; Yuan, D. Development of a protoplast isolation system for functional gene expression and characterization using petals of *Camellia Oleifera*. *Plant Physiol. Biochem.* **2023**, *201*, doi:10.1016/j.plaphy.2023.107885.
45. Li, S.; Zhao, R.; Ye, T.; Guan, R.; Xu, L.; Ma, X.; Zhang, J.; Xiao, S.; Yuan, D. Isolation, purification and PEG-mediated transient expression of mesophyll protoplasts in *Camellia oleifera*. *Plant Methods* **2022**, *18*, doi:10.1186/s13007-022-00972-1.

 doi:10.20944/preprints202512.2044.v1

46. He, X.; Xu, L.; Xu, X.; Yi, D.; Hou, S.; Yuan, D.; Xiao, S. Embryogenic callus induction, proliferation, protoplast isolation, and PEG induced fusion in *Camellia oleifera*. *Plant Cell, Tiss. Org.* **2024**, *157*, doi:10.1007/s11240-024-02800-x.
47. Li, Y., Wei, H., Yang, J., Du, K., Li, J., Zhang, Y., Qiu, T., Liu, Z., Ren, Y., Song, L., Kang X. High-quality de novo assembly of the *Eucommia ulmoides* haploid genome provides new insights into evolution and rubber biosynthesis. *Hortic. Res.* **2020**, *7*, 183.
48. Yang, Y.; Li, B.; Li, X.; Yuan, X.; Qu, B.; Wang, X.; Gao, X.; Fu, Y.; Gu, C. Deciphering the effects of *Endophytic Aspergillus* sp. Y232 on plant growth and the accumulation of characteristic bioactive compounds of *Eucommia ulmoides* Oliver. *J. Agric. Food Chem.* **2025**, *73*, 15014-15026, doi:10.1021/acs.jafc.4c12786.
49. Liu, J.; Cheng, T.; Wang, L.; Lian, C.; Ma, R.; Feng, W.; Lan, J.; Zhang, B.; Du, Q.; Kou, J.; et al. Genome-wide identification and comprehensive analysis of *EuFLS* genes in *Eucommia ulmoides* reveals their roles in growth, development, and abiotic stress response. *Front. Plant Sci.* **2025**, *16*, doi:10.3389/fpls.2025.1662635.
50. Chen, R., Namimatsu, S., Nakadozono, Y., Bamba, T., Nakazawa, Y., Gyokusen, K. Efficient regeneration of *Eucommia ulmoides* from hypocotyl explant. *Biol. Plant.* **2008**, *52*, 713-717. doi:10.1007/s10535-008-0137-x.
51. Xiao, S.; Tian, X.; Zhang, Y.; Wu, J.; Qin, C.; Wei, H.; Xie, S.; Yang, J.; Li, D.; Liu, Y. Development of *Eucommia ulmoides* Oliver tissue culture for in vitro production of the main medicinal active components. In Vitro *Cell. Dev. Pl.* **2024**, *60*, 548-560, doi:10.1007/s11627-024-10441-0.
52. Long, S.; Yang, J.; Wang, H.; Chen, X.; Zhao, D.; Zhao, Y. Genome-wide identification of *EuUSPs* in *Eucommia ulmoides* and the role of *EuUSP16* in rubber biosynthesis. *Front. Plant Sci.* **2025**, *16*, doi:10.3389/fpls.2025.1655155.
53. Zheng, L.; Zhao, D. Cloning and functional characterization of the legumin a gene (*EuLEGA*) from *Eucommia ulmoides* Oliver. *Sci. Rep.* **2024**, *14*, doi:10.1038/s41598-024-65020-5.
54. Yu,C.; Wang,L.; Chen,C.; He,C.; Hu,J.; Zhu,Y.; Huang,W. Protoplast: a more efficient system to study nucleo-cytoplasmic interactions. *Biochem. Biophys. Res. Commun.* **2014**, *450*, 1575-1580. doi: 10.1016/j.bbrc.2014.07.043.
55. Wang, L.; D,X.; Tan,A.; Zhao,D.; Zhao, Y. Optimization of regeneration system of transgenic *Eucommia ulmoides* Olive. *Seed* **2019**, *38*, 18-22,27.
56. Huang, S.; W, M.; Zhang, S. Rapid propagation technology of *Eucommia ulmoides* aseptic seedling tissue culture. *Mol. Plant Breed.* **2019**, *22*, 3045-3052.
57. Zhang, H.; H,Y.; Zhang, G.; Chen, S.; Wu, D.; Zhang, D.; Huang, G.; Zhang, B. Study on callus induction and proliferation culture technology of *Eucommia ulmoides* Oliv. *J Agr Sci Tech-IRAN.* **2019**, *21*, 157-162, doi:10.1334/j.nykjdb.2018.0386.
58. Zhang, S.; Ren, Y.; Wang, S.; Song, L.; Jing, Y.; Xu, T.; Kang, X.; Li, Y. EuHDZ25 positively affects rubber biosynthesis by targeting *EuFPS1* in *Eucommia* leaves. *Int. J. Biol. Macromol.* **2024**, *272*, doi:10.1016/j.ijbiomac.2024.132707.
59. Zhang, S.; Chen, H.; Wang, S.; Du, K.; Song, L.; Xu, T.; Xia, Y.; Guo, R.; Kang, X.; Li, Y. Positive regulation of the *Eucommia* rubber biosynthesis-related gene *EuFPS1* by EuWRKY30 in *Eucommia ulmoides*. *Int. J. Biol. Macromol.* **2024**, *268*, doi:10.1016/j.ijbiomac.2024.131751.
60. Cosgrove, D.J. Structure and growth of plant cell walls. *Nat. Rev. Mol. Cell Biol.* **2024**, *25*, 340-358, doi: 10.1038/s41580-023-00691-y.
61. David, H.; Laigneau, C.; David, A. Growth and soluble proteins of cell cultures derived from explants and protoplasts of *Pinus pinaster* cotyledons. *Tree Physiol.* **1989**, *5*, 497-506, doi: 10.1093/TREEPHYS/5.4.497.
62. Hu, B.; Dong, M.; Liu, R.; Shan, W.; Wang, Y.; Ding, Y.; Peng, J.; Meng, L.; Wang, C.; Zhou, Q. Establishment of an efficient protoplast isolation and transfection method for *Eucommia ulmoides* Oliver. *Front. Biosci. Landmark* **2024**, *29*, doi:10.31083/j.fbl2905187.
63. Russell, J.A. Advances in the protoplast culture of woody plants. *In Micropropagation of woody plant* **1993**, pp. 67-91, doi: 10.1007/978-94-015-8116-5_5.
64. Zeng, X.; Cao, X.; Zhao, Q.; Hou, S.; Hu, X.; Yang, Z.; Hao, T.; Zhao, S.; Yao, Z. Isolation of haustorium protoplasts optimized by orthogonal design for transient gene expression in *Phelipanche aegyptiaca*. *Plants* **2024**, *13*, 2163, doi:10.3390/plants13152163.

 doi:10.20944/preprints202512.2044.v1

65. Yao, L.; Liao, X.; Gan, Z.; Peng, X.; Wang, P.; Li, S.; Li, T. Protoplast isolation and development of a transient expression system for sweet cherry (*Prunus avium* L.). *Sci. Hortic.* **2016**, *209*, 14-21, doi: 10.1016/j.scienta.2016.06.003.
66. Nguyen, T.T.T.; Choi, N. Y.; Pyo, S. W.; Choi, Y. I.; Ko, J. H. Optimized and reliable protoplast isolation for transient gene expression studies in the gymnosperm tree species *Pinus densiflora*. *Forests*, **2025**, *16*, 1373. doi: 10.3390/f16091373.
67. Peng, Z.; Tong, H.; Liang, L.; Shi, Y.; Yuan, L. Protoplast isolation and fusion induced by PEG with leaves and roots of tea plant (*Camellia sinensis* L.O. Kuntze). *A. A. S.* **2018**, *44*, 463-470, doi: 10.3724/SP.J.1006.2018.00463.
68. Wang, Q.; Yu, G.; Chen, Z.; Han, J.; Hu, Y.; Wang, K. Optimization of protoplast isolation, transformation and its application in sugarcane (*Saccharum spontaneum* L). *Crop J.* **2021**, *9*, 133-142, doi: 10.1016/j.cj.2020.05.006.
69. Hou, S.; Li, Z.; Yi, D.; Wu, J.; Hu, Y.; Fan, X.; Yuan, D. Establishment of a system for tissue culture regeneration and isolation of *Camellia yubsienensis*, and PEG-mediated transient expression of mesophyll protoplasts. *Ind. Crops Prod.* **2024**, *222*, doi: 10.1016/j.indcrop.2024.119897.
70. Murashige, T.; Skoog, F. A revised medium for rapid growth and bio assays with tobacco tissue cultures. *Physiol. Plant.* **1962**, *15*, 473-497, doi:10.1111/j.1399-3054.1962.tb08052.x.
71. Li, L.; Zhang, T.; Lin, J.; Lian, X.; Zou, X.; Ma, X.; Wu, P. Longitudinal section cell morphology of Chinese fir roots and the relationship between root structure and function. *Front. Ecol. Evol.* **2023**, *11*, doi:10.3389/fevo.2023.1122860.